Target detection under sea background using constructed biorthogonal wavelet

Peng Zhang (张 鹏) and Jianxun Li (李建勋)

Automation Department, School of Electronic & Information and Electrical Engineering, Shanghai Jiao Tong University, Shanghai 200030

Received August 21, 2006

A new technique is presented to detect targets under sea background. Focused on interested areas, the spatial and frequency distributions are first studied, then analytic expression of targets is set up by least square method (LSM). According to the shape, frequency, and analytic expression of targets, a matched biorthogonal wavelet is constructed to better enhance targets and eliminate noises. Results show the usefulness of this method for single frame detection (signal to noise ratio SNR $\geq$ 1.25), which provides a better performance than classic wavelets and morphological filtering.

OCIS codes: 110.0110, 100.2000, 110.2970, 100.7410.

Target detection becomes tough when targets are small, weak and immersed in sea background with heavy waves and clutters. A basic way is to improve the performance of single frame detection, and wavelet transform has been proved to be a useful tool[1].

However, many famous orthogonal wavelets such as Harr and Daubechies, lacking desirable symmetry and linear phase — two critical factors in image processing, do not behave well due to slight shift[2]. Fortunately, biorthogonal wavelets bear the above properties and avoid shifting after transform. If the mother wavelet is similar to targets, the transform is considered as a matching filter detector and components of interests are thus easily to be detected. Therefore, targets need an in-depth studying.

An image derived form sea surface consists of four parts: sky, sea-sky line, sea surface, and land, where targets are submerged in waves and clutters, as shown in Fig. 1. High and dense gray level pixel areas are targets, waves, noises, and sand hills. The latter three items are leading roles influencing detection results.

Since the two-dimensional (2D) wavelet transform can be realized by two series-wound one-dimensional (1D) wavelet transforms, we only need to construct a 1D wavelet. Therefore, the vertical section of targets is to be well studied. To set up a correct expression of targets and thus construct a matched wavelet, statistic research is carried out with following findings: most targets are around 10×10 pixels area; its gray level distribution takes on a convex shape, and the vertical section appears a parabola shape, as shown in Figs. 2 and 3.

Sea background is concentrated on low frequency, clutters and noises on medium frequency, while targets on high frequency[3]. Combined with the gray level distribution, the joint distribution is drawn in Fig. 4.

Fig. 1. Image structure.

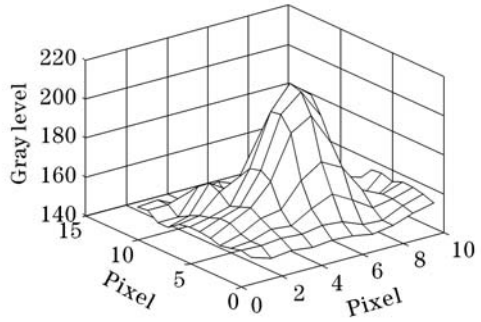

Fig. 2. Spatial shape of targets.

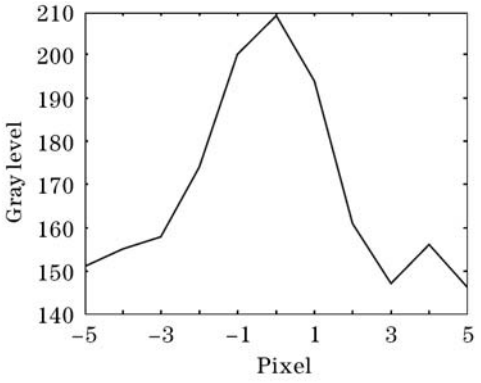

Fig. 3. Vertical section of targets.

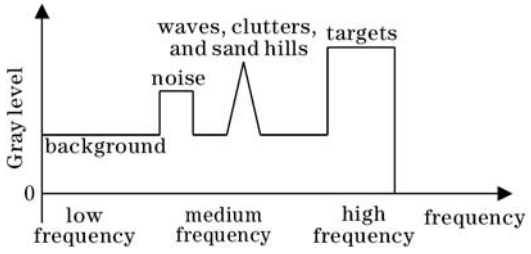

Fig. 4. Gray level and frequency distribution.

If a proper wavelet is constructed, the background can be mapped onto low frequency approximal version, noise and waves onto medium frequency version, while targets onto high frequency detail version. Consequently, every components in target areas are able to be separated and targets can thus be detected on a certain sub-frequency band.

Classical curve fitting method based on least square method (LSM) is used to set up the expression of targets' vertical section. Several targets are selected from sequence images as a set of samples $\{t_s\,|(x_j, y_j),\ j = \pm 5, \pm 4, \pm 3, \pm 2, \pm 1, 0\}$, where s is the sample number. In theory, the format of polynomial should be

$$f(x) = \sum_{n=0}^{b} a_n x^n, \quad (0 \le b \le 10). \tag{1}$$

In fact, the edge of target model (Fig. 2) is influenced by waves. Fluctuant edges should be cut off and the changed target model is given in Fig. 5, where target size is redefined as 7×7 pixels area $\{t_s\,|(x_j, y_j),\ j = \pm 3, \pm 2, \pm 1, 0\}$. Considering the boundary effect of high-order polynomial and the complexity of constructing high-order wavelets, the order is restricted as: $2 \le b \le 4$. Using LSM-based curve fitting method to process selected typical target samples, $b = 2$ is found to be best order. The analytic expression of target model is

$$f(x) = -5.87x^2 - 2.32x + 201.05, \tag{2}$$

and the outcome of curve fitting is shown in Fig. 5. According to the above expression, two-order B-spline function is selected as the basic wavelet to construct a matched basis.

Given the analysis and synthesis filters $h\,(k)$ and $g\,(k)$, scaling functions ϕ and $\widetilde{\phi}$ are defined as

$$\phi\,(t) = \sqrt{2} \sum_{k \in Z} h\,(k)\,\phi\,(2t - k), \tag{3}$$

$$\tilde{\phi}\,(t) = \sqrt{2} \sum_{k \in Z} \tilde{h}\,(k) \tilde{\phi}\,(2t - k)\,, \tag{4}$$

and wavelet ψ and its dual $\widetilde{\psi}$ are defined as

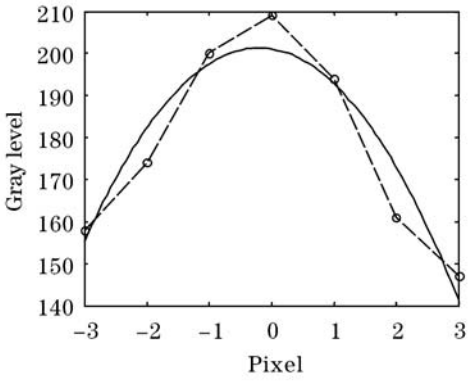

Fig. 5. Edge-removed vertical section.

$$\psi\,(t) = \sqrt{2} \sum_{k \in Z} g\,(k) \phi\,(2t - k)\,, \tag{5}$$

$$\tilde{\psi}\,(t) = \sqrt{2} \sum_{k \in Z} \tilde{g}\,(k)\,\tilde{\phi}\,(2t - k), \tag{6}$$

where $g(k) = (-1)^k\,\tilde{h}_{1-k}$, $\tilde{g}(k) = (-1)^k\,h_{1-k}$, $k \in Z$.

The two wavelets are duals of each other, and the wavelet families are biorthogonal:

$$\left\langle \phi_{j,k}, \tilde{\phi}_{j,n} \right\rangle = \delta_{k,n}, \quad \text{and} \quad \left\langle \psi_{j,k}, \tilde{\psi}_{m,n} \right\rangle = \delta_{j,m}\delta_{k,n}. \tag{7}$$

Using two different wavelet bases, ψ and $\widetilde{\psi}$, one for decomposition and the other for reconstruction, symmetrical wavelets with compact support are obtained.

Let $H(w) = \frac{1}{\sqrt{2}} \sum\limits_{k \in Z} h_k \mathrm{e}^{-ikw}$ and $\widetilde{H}(w) = \frac{1}{\sqrt{2}} \sum\limits_{k \in Z} \widetilde{h}_k \mathrm{e}^{-ikw}$. Transfer functions of ϕ, $\widetilde{\phi}$ are $\widehat{\phi}(w) = \prod\limits_{j=1}^{+\infty} H\left(\frac{w}{2^j}\right)$ and $\widehat{\widetilde{\phi}}(w) = \prod\limits_{j=1}^{+\infty} \widetilde{H}\left(\frac{w}{2^j}\right)$, then the following equations can be proved,

$$H(w)\overline{\widetilde{H}(w)} + H(w+\pi)\overline{\widetilde{H}(w+\pi)} = 1$$

$$\Leftrightarrow \sum_{k \in Z} h_k \widetilde{h}_{k+2n} = \delta_{n0}. \tag{8}$$

$H(w)$ and $\widetilde{H}(w)$ are supposed to be

$$H(0) = \widetilde{H}(0) = 1, \quad H(\pi) = \widetilde{H}(\pi) = 0. \tag{9}$$

Thus lowpass filters $\{h_k\}$ and $\left\{\widetilde{h}_k\right\}$ meet

$$\begin{cases} \sum\limits_k h_{2k} = \sum\limits_k h_{2k+1} = 1 \\ \sum\limits_k \widetilde{h}_{2k} = \sum\limits_k \widetilde{h}_{2k+1} = 1 \end{cases}. \tag{10}$$

In the light of two scaling functions and Eq. (7), the condition on $j = 0, 1$ can be deduced:

$$\left\langle \phi_{0l}, \widetilde{\phi}_{0k} \right\rangle = \sum_k h_n \widetilde{h}_n (\phi_{1l}, \widetilde{\phi}_{1k}) = \delta_{lk}, \tag{11}$$

$$\left\langle \phi_{1l}, \widetilde{\phi}_{1k} \right\rangle = \delta_{lk}/2. \tag{12}$$

Therefore, $\left\{\widetilde{h}_n\right\}$can be figured out if only $\{h_n\}$ is given, and thus dual scaling functions can be constructed. According to Eqs. (5) and (6), wavelets ψ and its dual $\widetilde{\psi}$ are obtained[4].

B-spline wavelets were introduced by Chui[5]. Any multi-dimensional scaling function of order γ can be represented as the convolution of a polyharmonic B-spline of order γ and a distribution with a bounded Fourier transform[6,7]. Based on the shape and order of the analytic expression of target model Eq. (2), the two-order B-spline function is selected as the mother wavelet.

The m degree B-spline scaling function N_m is defined

as

$$N_m(x) = N_1 * N_{m-1} = \int_{-\infty}^{+\infty} N_1(t) N_{m-1}(x-t)\mathrm{d}t$$

$$= \int_{-\frac{1}{2}}^{\frac{1}{2}} N_{m-1}(x-t)\mathrm{d}t \qquad (m = n+1), \tag{13}$$

$$N_1(x) = \begin{cases} 1, & -\frac{1}{2} \le x \le -\frac{1}{2} \\ 0, & \text{otherwise} \end{cases}. \tag{14}$$

Thus the 2th B-spline (i.e. 3 degree B-spline) scaling function is deduced as

$$\phi(x) = N_3(x) = \begin{cases} \frac{(x+1)^2}{2}, & -1 \le x \le 0 \\ -(x-\frac{1}{2})^2 + \frac{3}{4}, & 0 \le x \le 1, \\ \frac{(x-2)^2}{2}, & 1 \le x \le 2, \\ 0, & \text{otherwise} \end{cases}. \tag{15}$$

Scaling function $\phi(x)$ satisfies the two-scaling function:

$$\phi(t) = \frac{1}{4}\phi(2t+1) + \frac{3}{4}\phi(2t) + \frac{3}{4}\phi(2t-1) + \frac{1}{4}\phi(2t-2). \tag{16}$$

Its Fourier transform is $\hat{\phi}(w) = (2\pi)^{-\frac{1}{2}} \mathrm{e}^{-\frac{iw}{2}} \left(\frac{\sin(\frac{w}{2})}{\frac{w}{2}}\right)^3$. Thus

$$2\pi \sum_k \left|\hat{\phi}(w+2\pi k)\right|^2 = \frac{8}{15} + \frac{13}{30}\cos w + \frac{1}{30}\cos^2 w. \tag{17}$$

Obviously, $\phi \in L^1$ and $\int_R \phi(x)\mathrm{d}x \neq 0$. It can be proved that $\{\phi(x-k)\}_{k\in Z}$ are the Riesz basis of V_0. Detailed derivation and testimony can be seen from Ref. [8]. Let $g_{mk} = (-1)^k h_{m,1-k}$, thus the m degree B-spline wavelet ψ_m is defined as

$$\psi_m(x) = \sqrt{2} \sum_{k\in Z} g_{mk} \phi_m(2x-k). \tag{18}$$

According to Eq. (16), the number of lowpass filters is four. The number of its dual can be calculated as eight by Eqs. (11) and (12). Let $\{h_n\}_{-1}^{2}$ and $\left\{\widetilde{h}_n\right\}_{-3}^{4}$ represent the coefficients of ϕ and $\widetilde{\phi}$, the two-scaling function and its dual are written as

$$\phi(t) = h_{-1}\phi(2t+1) + h_0\phi(2t) + h_1\phi(2t-1) + h_2\phi(2t-2), \tag{19}$$

$$\widetilde{\phi}(t) = \widetilde{h}_{-3}\phi(2t+3) + \widetilde{h}_{-2}\phi(2t+2) + \widetilde{h}_{-1}\phi(2t+1) + \widetilde{h}_0\phi(2t) + \widetilde{h}_1\phi(2t-1) + \widetilde{h}_2\phi(2t-2) + \widetilde{h}_3\phi(2t-3) + \widetilde{h}_4\phi(2t-4). \tag{20}$$

The values of lowpass filter are already symmetrical in fact, i.e., $h_{-1} = h_2 = \frac{1}{4}$, $h_0 = h_1 = \frac{3}{4}$.

Then set its dual filter satisfy the symmetrical condition:

$$\widetilde{h}_{-3}=\widetilde{h}_4, \quad \widetilde{h}_{-2} = \widetilde{h}_3, \quad \widetilde{h}_{-1} = \widetilde{h}_2, \quad \widetilde{h}_0 = \widetilde{h}_1. \tag{21}$$

Based on Eq. (10)—(12), (19), and (20), the dual filter is then obtained:

$$\widetilde{h}_1 = \frac{3}{2} + \frac{\widetilde{h}_3}{3}, \quad \widetilde{h}_2 = -\frac{1}{2} - \widetilde{h}_3, \quad \widetilde{h}_4 = -\frac{\widetilde{h}_3}{3}, \tag{22}$$

where $\widetilde{h}_3$ is a free variable. Thus the coefficients of biorthogonal wavelet can be selected adaptively according to analytic expression of targets or features of images. Here let $\widetilde{h}_3 = -0.27$, and the coefficients of dual filter are computed through Eqs. (21) and (22),

$$\widetilde{h}_{-3} = 0.09, \quad \widetilde{h}_{-2} = -0.27, \quad \widetilde{h}_{-1} = -0.23, \quad \widetilde{h}_0 = 1.41,$$

$$\widetilde{h}_1 = 1.41, \quad \widetilde{h}_2 = -0.23, \quad \widetilde{h}_3 = -0.27, \quad \widetilde{h}_4 = 0.09.$$

To prove the usefulness of this method, 480×640 infrared images were obtained from real sea condition. Target in Fig. 6(a) takes on a convex shape, and Fig. 7(a) a concave one. Though energy within target area is weak, its peak value is still higher than its surroundings in Fig. 6(a). Biorthogonal wavelet is constructed to this case. Therefore, as for concave targets in Fig. 7(a), images are

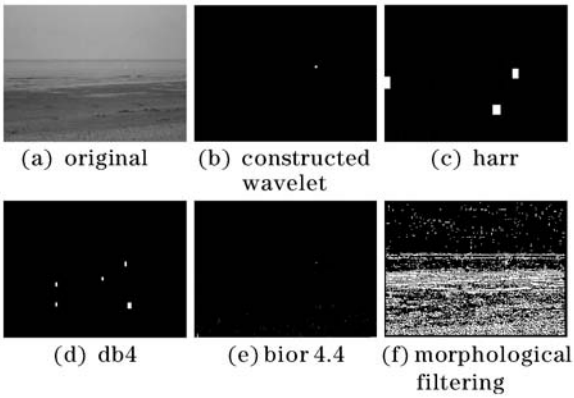

Fig. 6. Results by different wavelet bases (SNR = 1.25).

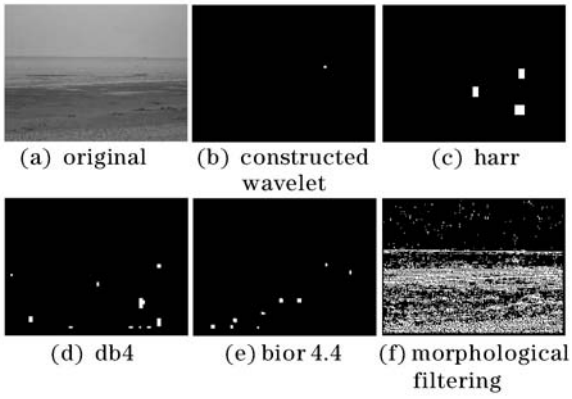

Fig. 7. Results by different wavelet bases (SNR = 1.73).

first processed by complement operation. Set the decomposition order to be five, which provides favorable subfrequency in practice, and carry out the common gray-level thresholding for segmentation. Meanwhile, using harr, db4, bior4.4, and morphological filtering to process images, comparisons can be drawn from Figs. 6 and 7, where signal to noise ratio (SNR) of the original image is defined as SNR $= \frac{S-N}{\sigma}$, S is the mean gray level of target, N is the mean gray level of the image, and σ is the standard deviation of the image.

Obviously, the constructed biorthogonal wavelet performs better than others. Harr function detected the target at the cost of amplifying the original size of targets. This maybe result from its short compact support compared to target size. Db4 failed to suppress the great influence generated by waves and sand hills. Though bior4.4 is biorthogonal, its compact support is relatively long compared to targets' size. Only part of target can be detected mixed with many noises. Morphological filtering proves to be worst here. It operates only on spatial-domain thus cannot make use of the differences between targets and becomes noised in frequency-domain.

In conclusion, we studied spatial and frequency features of targets, and built up analytic expression of targets based on which a similar mother wavelet is selected and a matched biorthogonal wavelet is constructed. Coefficients of dual filters are set to be symmetrical thus little but important information within target area is enhanced after wavelet transform. This method provides the good performance consistent with theoretical prediction. It is able to detect targets correctly and suppress noises at the same time, which lays solid foundation for the following multi-frame detection and tracking.

This work was jointly supported by the China Aviation Science Foundation (No. 03F57003), the National Natural Science Foundation of China (No. 60304007), and the National Key Laboratory Science Foundation (No. 51476010604JW0303). P. Zhang's e-mail address is pengz@sjtu.edu.cn.

References

1. C. Li, Y. Wei, and Z. Shi, in *Proceedings of IEEE International Conference on Robotics, Intelligent Systems and Signal Processing* 1191 (2003).
2. E. P. Simoncelli, W. T. Freeman, E. H. Adelson, and D. J. Heeger, IEEE Trans. Information Theory **38,** 587 (1992).
3. Y.-S. Moon, T. Zhang, Z. Zuo, and Z. Zuo, Int. J. Pattern Recognition & Artifical Intelligence **14,** 907 (2000).
4. Y. Li and C. Xu, J. Huazhong Univ. Sci. Tech. (Nature Science Edition) **34,** 37 (2005).
5. C. T. Chui, *An Introduction to Wavelets* (Academic Press, San Diego, 1992).
6. M. Unser and T. Blu, Proc. SPIE **5207,** 147 (2003).
7. T. Blu and M. Unser, in *Proceedings of IEEE International Conference on Acoustics, Speech, and Signal Processing* VI-421 (2003).
8. M. Liu, *Wavelet Analysis and Its Application* (Tsinghua University Press, Beijing, 2005) Chap.5, 6.